ENGINEERING TRANSACTIONS • *Engng. Trans.* • **52**, 1-2, 71–90, 2004
Polish Academy of Sciences • Institute of Fundamental Technological Research
10.24423/engtrans.470.2004

MATERIAL NONLINEAR ANALYSIS OF PLANE STRUCTURES MADE OF CEMENT BASED COMPOSITE MATERIALS USING THE ANSYS SYSTEM

J. Pencik

Brno University of Technology
Faculty of Civil Engineering, Institute of Structural Mechanics,
Veveri 95, 662 37 Brno, Czech Republic
e-mail: pencik.j@fce.vutbr.cz

At present, it is possible to carry out a structure analysis using various calculation systems based mainly on the Finite Element Method (FEM). These systems mostly include finite elements, which can be used for geometrical and material nonlinear analysis of civil-engineering structures. Most of these elements are derived and used especially for the analysis of steel structures. For the analysis of structures made of cement based composite materials are developed and special elements are used. The article describes the methods of analysis of structures made of cement based composite materials with respect to material non-linearity. The ANSYS analysis system is further described in the article and the beam element implemented in this system.

The beam element detailed derivation, including the presentation of material models that can be used for an analysis with this element is presented. Some numerical examples are shown at the end of the article.

Key words: FEM, FEA, nonlinear analysis, reinforced concrete, plane, beam element, ANSYS.

1. Introduction

The current state of computer technology and programs enables the solution of both statically and dynamically loaded civil-engineering structures, taking into account the effects of material, geometric and structural non-linearity. These analyses could also include the rheological properties of materials such as, for example, the analysis of bridge structures made with the use of TDA system [22, 23] or TDV system [25] etc. To model structures made of cement-based composite materials, special finite elements and material models are generated for the FEM [8, 15, 18, 20, 21]. These special elements have the ability to include many effects important for both the quality of the design and the

evaluation of complex framed, shell and three-dimensional structures. For the development of two-dimensional or three-dimensional analysis, models of some civil-engineering structures in applied design work, for example bridges, towers, industrial assembly halls etc., beam elements, are mainly utilized.

Today, to analyze the civil-engineering structures, a designer can use several analysis systems, for example ABAQUS, ANSYS, MARC, NASTRAN, COSMOS, SBETA, ATHENA, NEXIS 32/TDA, TDV etc.

Of the mentioned analysis systems, ANSYS [3] is widely used all over the world. The system is employed in engineering offices and also used for education of students at technical universities. The system can also be used in the design of civil-engineering structures and especially mechanical constructions and machine components. For the solution of material nonlinear problems, the ANSYS system provides several beam elements (BEAM23, BEAM24, BEAM44), shell elements (SHELL43, SHELL93) and solid elements (SOLID45, SOLID65, SOLID92, SOLID95) [1]. For material nonlinear calculations made by means of the mentioned elements, there is a relatively wide range of material models to be used, based on the rate-independent plasticity, rate-dependent plasticity, creep, swelling, nonlinear elasticity, hyperelasticity and viscoelasticity. With the use of these material models and standard elements, material models of cement-based composite materials can not be defined, mainly because it is impossible to model softening in the tensile part of the material models (stress-strain diagrams) or material models that use fracture mechanics for description of construction behaviour before and after its rupture (description of crack propagation). Unlike the "traditional" elements for nonlinear material analysis, the ANSYS system allows the utilization of "layered" elements – a shell element (SHELL91) and a three-dimensional element (SOLID191). These elements can be used for the calculation of layered composite structures involving materially nonlinear behaviour and using the above mentioned material models.

For modelling plane, reinforced concrete and prestressed structures, i.e. structures made of cement-based composite materials, the ANSYS system provides only one three-dimensional element (SOLID65), which uses the material model of concrete according to WILLIAM and WARNKE [2]. The beam elements used for modelling reinforced concrete and prestressed structures are not included in the ANSYS system. For this reason, it is appropriate to incorporate special beam elements together with the material models into the ANSYS library of elements and material models.

2. MATERIAL NON-LINEARITY

Nonlinear problems generally result from material equations following the respective nonlinear dependence between the stress vector $\{\sigma\}$ and strain vec-

tor $\{\varepsilon\}$, which, if we consider the influence of temperature and shrinkage etc., is reduced by the vector of the initial deformation $\{\varepsilon_0\}$; this means that the stress is a nonlinear function of the strain. This relationship, which is path-dependent, so that the stress depends on the strain history as well as on the strain itself, can be written using the stiffness matrix of the material $[D]$, whose terms are generally dependent on the components of deformation and on time, as follows:

$$\{\sigma\} = [D] \cdot (\{\varepsilon\} - \{\varepsilon_0\}) . \tag{2.1}$$

The linear or nonlinear behaviour of the material in Eq. (2.1) is described by the stiffness matrix of material $[D]$. If the material behaviour is linear elastic, the stiffness matrix of material $[D]$ is symmetric and is called elastic. The border between the linear elastic behaviour of the material and the plastic behaviour is determined by the surface of plasticity, i.e. the condition of plasticity. Depending on the material type, the surface of plasticity may remain constant or it may change. For example, if the material exhibits hardening, the surface of plasticity increases depending on the load history [5]. To describe the behaviour of the material, a number of conditions of plasticity can be used, for example those of Drucker–Prager, Mises, Mohr–Coulomb, Mises–Huber–Hencky, Tresca, Hoffman, Chen, Kupfer, Hill, William and Warnke, etc. To describe the deformational characteristics of concrete or materials that have different tensile and compressive plasticity limits, it is possible to use the Drucker–Prager, Chen, Kupfer, William–Warnke, etc. conditions. If the material can be defined in terms of the Drucker-Prager stability postulate as stable, then the stiffness matrix of material $[D]$ can be called elasto-plastic and it is symmetric and includes the associated law of the plastic transformation. Otherwise, e.g. with materials with internal friction [2], which are not connected with the Drucker–Prager stability postulate, the elasto-plastic stiffness matrix of material $[D]$ is asymmetric and contains non-associated law of the plastic transformation.

Equation (2.1) of nonlinear dependence between the stress vector σ and strain vector ε is preferred especially in calculations and integration of the elements for materially nonlinear systems. In these systems, as well as in the ANSYS system, the analysis of Eq. (2.1) is usually done using the method of incremental strains. The procedure for the calculation can be summarized in the following points [2, 9, 10]: (i) computation of incremental displacements, (ii) updating of incremental displacements from the last converged equilibrium state, (iii) computation of the incremental strains from incremental displacements, (iv) computation of incremental stresses, (v) updating of the stresses and (vi) computation of internal forces.

To solve materially nonlinear problems using Eq. (2.1), it is necessary to define and describe the material characteristic and, above all, to clarify the nonlinear character of the material models (possible dissimilarities in the tensile and

compressive behaviour of the material), the possibility of unloading and recurring loading, etc. For concrete (plain, reinforced and prestressed), which is classified as a non-homogeneous material, it is useful to consider in the calculation its imperfections such as pores, air voids, lenses of water under coarse aggregates, shrinkage cracks, etc., which originate in the material before its mechanical loading and also the failures originating during the external loading. Generally, the material models used to describe the behaviour of materials in non-linear analysis can be divided into (i) material models based on the theory of plasticity, (ii) material models based on the principles of fracture mechanics and (iii) cohesive fracture material models.

Models that follow the theory of plasticity are based on the stress or strain failure criterion; this means that only the ultimate stress or the ultimate strain determines the failure of the material. These material models are used in most national codes and regulations, for example in EC 2, CEB-FIP MC 90, CSN, ÖN, DIN, etc. As for concrete, the material models presently used to design concrete structures do not enable exploitation of the tensile carrying capacity of concrete, because most of them consider only the possibility of compressive stress of concrete, i.e. the tensile part of the material model is not defined. This shortcoming is removed by models using fracture mechanics for the description of the material behaviour. These models are based on the energy failure criterion. The models enable the description of the behaviour of the material after reaching the ultimate stress or the ultimate strain that results in the formation of cracks. At the same time, they enable specification of the way in which these cracks are going to propagate in the structure. Other types of material models are cohesive fracture models, which are based on the cohesion theory. This theory considers fracture to be a gradual process in which separation between incipient material surfaces is resisted by cohesive tractions. The models can be used to describe and predict the fracture processes occurring in engineering materials loaded in tension.

3. Material nonlinear analysis of plane structures

For material nonlinear analysis of structures made of cement-based composite materials, the ANSYS program system is used with the beam element and material models. The element, which assumes uniaxial state of stress and material models, is implemented into the ANSYS library of elements and material models.

To model the supporting elements of civil-engineering structures, e.g. reinforced concrete girders prestressed by tendons, the "adapted layered" approach is used, Fig. 1. In this approach the supporting elements are, in the longitudinal direction, divided by vertical sections into a finite number of structural parts. In each structural part, the concrete cross-section is vertically divided into a finite

number of parts, so-called layers, while reinforcement and tendons are usually considered as one unit. Each concrete layer, reinforcement and tendon is modelled separately as an individual beam element. This is the basic difference between the "classical layered" and "adapted layered" approaches. In the case of "classical layered" approach, the structural part is modelled as one beam element.

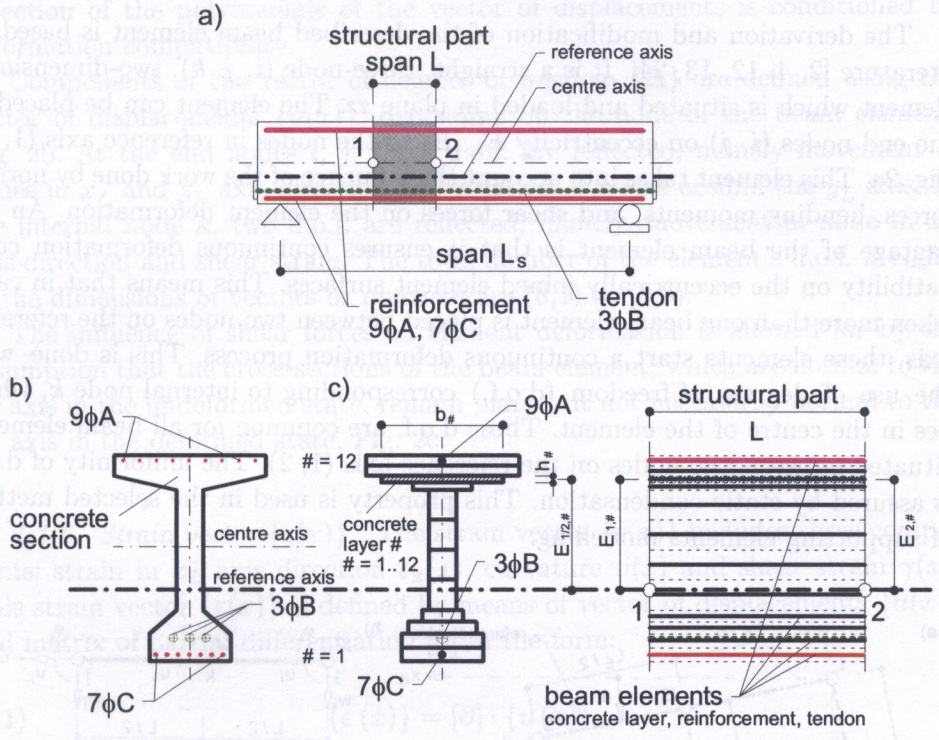

FIG. 1. Structure modelling – longitudinal section (a), real cross-section (b), cross-section and longitudinal section in case of the use of "adapted layered" approach (c).

4. BEAM ELEMENT

Civil-engineering structures include a variety of supporting elements (girders, columns, reinforcement, tendons, etc.) that can be made of various materials (ceramics, masonry, concrete, reinforcement, prestressing steel, etc.). For these reasons, when choosing an element for the analysis of these structures, it is advisable to choose one which enables modelling of all the previously mentioned types of materials and supporting elements.

An example of a two-dimensional beam element which can be used for modelling the mentioned types of materials and supporting elements, is that which is used in the TDA modulus of the NEXIS 32 system [14]. After modification and

completion of this element, it is possible to use it for material nonlinear analysis together with the material models in the ANSYS system described below.

4.1. Beam element description

The derivation and modification of the described beam element is based on literature [2, 4, 12, 13, 24]. It is a straight, three-node (i, j, k), two-dimensional element which is situated and loaded in plane xz. The element can be placed at the end nodes (i, j) on eccentricity E_1, E_2 to the nodes in reference axis (1, 2), Fig. 2a. This element takes into account the influence of the work done by normal forces, bending moments, and shear forces on the element deformation. An advantage of the beam element is that it ensures continuous deformation compatibility on the eccentrically joined element surfaces. This means that in cases when more than one beam element is placed between two nodes on the reference axis, these elements start a continuous deformation process. This is done with the use of degrees of freedom (d.o.f.) corresponding to internal node k, which lies in the centre of the element. These d.o.f. are common for all beam elements situated between two nodes on the reference axis (1, 2). The uniformity of d.o.f. is assured by static condensation. This property is used in the selected method of supporting elements modelling.

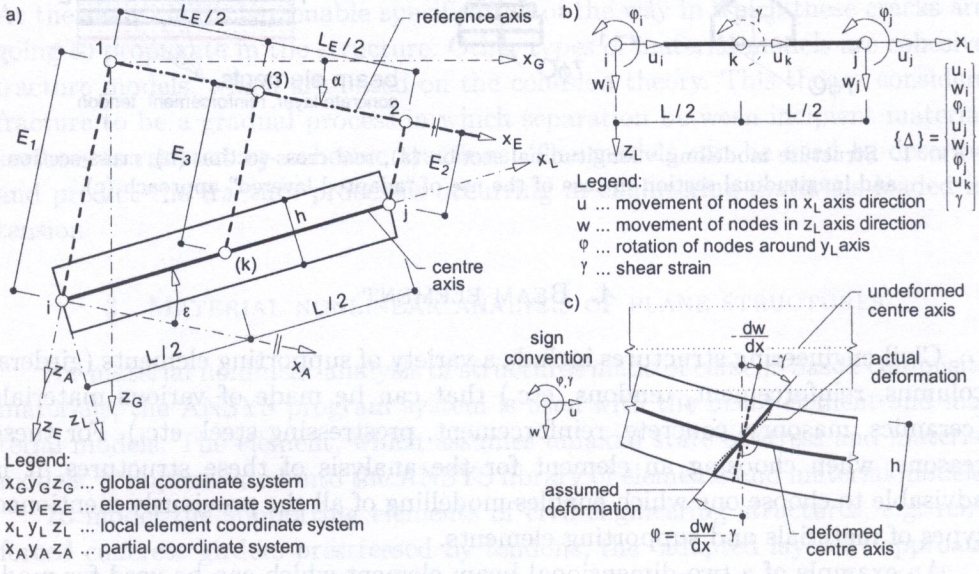

FIG. 2. Beam element with coordinate systems (a), vector of degrees of freedom $\{\Delta\}$ and its components (b), longitudinal section before and after element's deformation (c).

4.1.1. Vector of displacements $\{u(x)\}$ *and vector of degrees of freedom* $\{\Delta\}$. The vector of displacements $\{u(x)\}$ of a beam element includes three components: $u(x)$ – displacement of nodes in x_L axis direction (second degree polynomial), $w(x)$ – displacement of nodes in z_L axis direction (third degree polynomial) and $\gamma(x)$ – shear strain (zero degree polynomial); $\{u(x)\} = \{u(x), w(x), \gamma(x)\}^T$. Selection of the polynomials of the vector of displacements is conditioned by deformation compatibility.

Components of the vector of degrees of freedom $\{\Delta\}$ are defined using the vector of displacements $\{u(x)\}$, depending on the node of the beam element, Fig. 2b. At the end nodes i, j, three d.o.f. are reflected, namely movement of nodes in x_L and z_L axis direction and rotation of nodes around the y_L axis. In the internal node k, two d.o.f. are reflected, namely, movement of node in x_L axis direction and shear strain. The total number of the element's d.o.f. is eight, so the dimensions of vectors or matrices are (8,1) or (8,8).

The influence of shear forces on element deformation is allowed for by the assumption that the cross-sections of the beam element, which are normal to the x_L axis in the undeformed state, remain plane but not necessarily normal to the x_L axis in the deformed state, Fig. 2c.

4.1.2. Strain vector $\{\varepsilon(x)\}$. The strain vector $\{\varepsilon(x)\}$ includes three components: strain in x_L axis direction $\varepsilon_x(x)$, curvature $\upsilon(x)$ and shear strain $\gamma(x)$. This strain vector $\{\varepsilon(x)\}$ is defined by means of vector of displacements $\{u(x)\}$ and matrix of partial differentiation $[\partial]$ in the form:

$$\{\varepsilon(x)\} = [\partial] \cdot \{u(x)\}, \tag{4.1}$$

where $\{\varepsilon(x)\} = \{\varepsilon_x(x), \upsilon(x), \gamma(x)\}^T$, $[\partial] = \operatorname{diag}[\partial/\partial x, \partial^2/\partial x^2, 1]$ and $\{u(x)\} = \{u(x), w(x), \gamma(x)\}^T$.

4.1.3. Stiffness matrix $[K]$. The stiffness matrix $[K]$ is derived from the potential energy of the internal forces in the form:

$$[K] = \int_L [N]^T \cdot [\partial]^T \cdot [D] \cdot [\partial] \cdot [N] \, dx, \tag{4.2}$$

where $[D]$ is the stiffness matrix of the material including the cross-sectional characteristics; $[D] = \operatorname{diag}[EA, EI, GA_T]^T$ (A is cross-sectional area, A_T is cross-sectional area reduced by shear factor and I is moment of inertia) and $[N]$ is the matrix of the shape functions.

4.1.4. Mass matrix $[M]$. The mass matrix $[M]$ is derived in the consistent and lumped form [2]. Both forms are defined using density ρ, which is considered to be constant along the length of the element, by the formula:

$$[M] = \rho \iiint_V [N]^T \cdot [N] \, dV. \tag{4.3}$$

For mass matrix in the consistent shape, it is assumed that all components of the mass matrix are considered, but for mass matrix in the lumped form only the diagonal components are considered.

4.1.5. Vector of internal forces $\{\sigma(x)\}$. The vector of internal forces consists of normal force $N(x)$, shear force $V(x)$ and bending moment $M(x)$; $\{\sigma(x)\} = \{N(x), V(x), M(x)\}^T$. This vector can be expressed by the stiffness matrix of the material $[D]$ and the strain vector $\{\varepsilon(x)\}$ or after the adaptation by matrix of partial differentiation $[\partial]$, matrix of shape functions $[N]$ and vector of degrees of freedom $\{\Delta\}$, as follows:

$$\{\sigma(x)\} = [D] \cdot \{\varepsilon(x)\} = [D] \cdot [\partial] \cdot [N] \cdot \{\Delta\}. \tag{4.4}$$

The calculation of Eq. (4.4) is done by the method of incremental strains. The resulting internal forces are obtained by integration over the volume V of the element. The integration is carried out using numerical methods – for integration over the element's length, the Gauss three points quadrature is used and for integration over the element's cross-section, the five point Newton–Cotes method is used.

The pattern of internal forces along the element's length depends on the selected substitutive polynomials of the vector of displacements $\{u(x)\}$ and on provision of continuous deformation compatibility on the eccentrically joined element surfaces, and it is done by use of the d.o.f. corresponding to the internal node k (u_k, γ). These d.o.f. are common to every element situated between two nodes on the reference axis, Fig. 1c. The uniformity of the d.o.f. is assured by static condensation. Due to the condensation, the resulting pattern of the normal force is constant, the bending moment is linear and the shear force is also constant along the element's length. The influence of static condensation is displayed also in the change of size of the matrices and vectors whose dimensions before the condensation were (8,8) – $[K]$, $[M]$ or (8,1) – $\{\Delta\}$, while after the condensation their dimensions are (6,6) or (6,1).

4.2. Material and rheological models

The material nonlinear analysis of structures made of cement based composite materials using the described beam element can be applied for the real

behaviour modelling of materials (concrete, reinforcement, tendons, masonry, ceramic blocks, etc.). Derivation of the material models is based on the requirement of the most general process of set-up, i.e. possibility of standard material models set-up or material models obtained from experimental tests.

To model the reinforcement or tendon and concrete behaviour it is possible to use multi-linear material models defined by general points of coordinates $[\varepsilon_i;\ \sigma_i]$ for $i = 1$ to number of general points, Fig. 3, 4. An advantage of this definition is the possibility of modelling the material models described in the national codes and also models obtained from experimental tests.

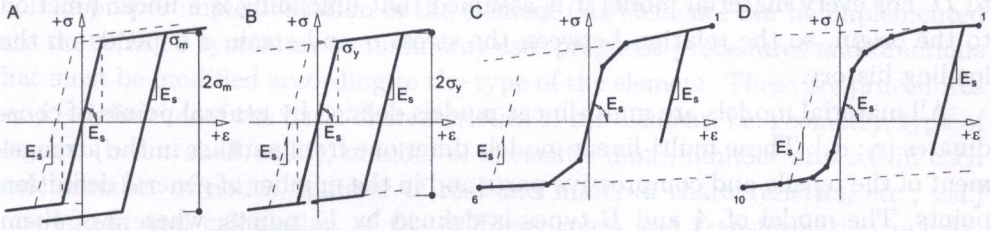

FIG. 3. Material models of reinforcement and tendon.

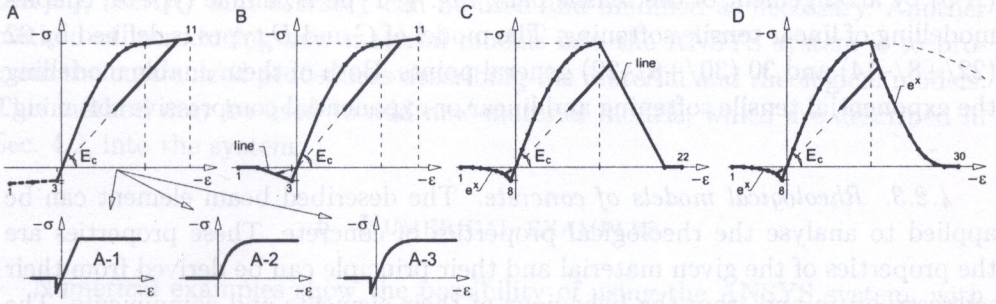

FIG. 4. Material models of of concrete.

4.2.1. Material models of reinforcement and tendon. For modelling the reinforcement and tendon behaviour it is possible to use four types of material models indicated in Fig. 3 as types A to D. For every material model it is assumed that the unloading path is parallel to the tangent leading through the origin of the material model.

The material model of type A is a bilinear isotropic material model built up according to [4], which uses the Mises condition of plasticity with the associated law of plastic deformation and with the isotropic criteria of strengthening ($2\sigma_m$).

The material model of type B is a bilinear kinematic material model which utilizes the Mises condition of plasticity with the associated law of plastic deformation ($2\sigma_y$). The material models of type C and D are multi-linear models defined by general points of coordinates $[\varepsilon_i; \sigma_i]$. These two material models are defined by 6 or 10 general points, which can be obtained from experimental testing. All models enable modelling of tensile and compressive hardening.

4.2.2. Material models of concrete. To model the behaviour of concrete, it is possible to use four types of material models indicated in Fig. 4 as type A to D. For every material model it is assumed that unloading is a linear function to the origin, so the relation between the stress σ and strain ε depends on the loading history.

All material models are multi-linear models defined by general points of coordinates $[\varepsilon_i; \sigma_i]$. These multi-linear models differ one from another in the arrangement of the tensile and compressive parts and in the number of general definition points. The model of A and B types is defined by 11 points, where 3 of them define the tensile and the others-the compressive parts of the model, indicated (11/+3/–8). Using the model of type A it is possible to define the material models described in national codes, e.g. CSN (A-1), EC 2 (A-2) a CEB-FIP MC 90 (A-3) by arrangement of the tensile part, Fig. 4. Type B, unlike type A, enables modelling of linear tensile softening. The model of C and D types is defined by 22 (22/+8/–14) and 30 (30/+8/–22) general points. Both of them enable modelling the exponential tensile softening and linear or exponential compressive softening.

4.2.3. Rheological models of concrete. The described beam element can be applied to analyse the rheological properties of concrete. These properties are the properties of the given material and their principle can be derived from their microstructure and from the behaviour of their elements and components. The behaviour of the rheological properties (creep, shrinkage) can cause an enlargement in the structure's deformations and redistribution of the stress among the individual supporting elements or among parts of the cross-section or the whole structure. To analyse the influence of the rheological properties on the structures it is necessary to apply a numerical method, for example time-dependent method in combination with the FEM. The time-dependent method is based on the successive calculation of the structures in discrete times called time nodes, into which the full interval analysed is divided. If the principle of viscoelasticity theory is valid, the given problems can be solved using the time dependent method in combination with the FEM. All changes of the structure configuration (progressive assembly, tension of prestressing tendons, change of static system, etc.) have to be respected in the analysis.

For modelling of the rheological properties of concrete it is possible to use models which are specified in the national codes CSN 73 1201-86 and CSN P ENV 1992-1-1.

4.3. Implementation into the ANSYS

The problems of implementation of elements and material models into the ANSYS system are described in detail in references [2, 16, 17]. To introduce new components and functions into the ANSYS system, the standard programming languages Microsoft C++ and Compaq Visual Fortran have to be used.

The proper implementation of the element (six elements can be implemented into the ANSYS system as a maximum) uses prepared procedures and functions that must be modified according to the type of the element. These are procedures *uec.f* – definition of the basic characteristics of the element, i.e. geometry, type of element (beam/shell/solid), number of element's d.o.f., number of d.o.f. in each node, number of nodes, number of real and material characteristics, etc.; *uel.f* – definition and calculation of the stiffness, mass and transformation matrix, internal forces, etc. The complete contents including all the available procedures is listed in [2].

To integrate the material and rheological models, the prepared procedures *userpl.f*, *usercr.f* and *usersw.f* can be used and modified as necessary. Another method of introducing new material models into the ANSYS system is to program the customized procedures describing the material and rheological models. This method may be used to add new material models, which are described in Sec. 4.2, into the system.

5. Numerical examples

Numerical examples show the possibility of using the ANSYS system, with the described beam element and material models, for material non-linear analysis. In these examples, the calculated results are compared with the results available in literature and with the results obtained by means of the standard ANSYS elements.

5.1. Example No. 1

Numerical example No. 1 describes modelling of the three-point bending test for a simply supported steel girder, which is introduced in [15]. The simply supported girder of rectangular cross-section $b \times h = 0.15 \times 0.30$ m and span $L = 3.00$ m is loaded at mid-span (at point A) by vertical force F, the value of which is changed during the computation. The height h of the cross-section is divided into 6 layers, Fig. 5, ($A_T = 0.833 \times A$). The real material behaviour

is described as in [15] using the material model of type A without hardening ($E = 210\,\text{GPa}$; $\mu = 0.3$; $\sigma_y = 250\,\text{MPa}$).

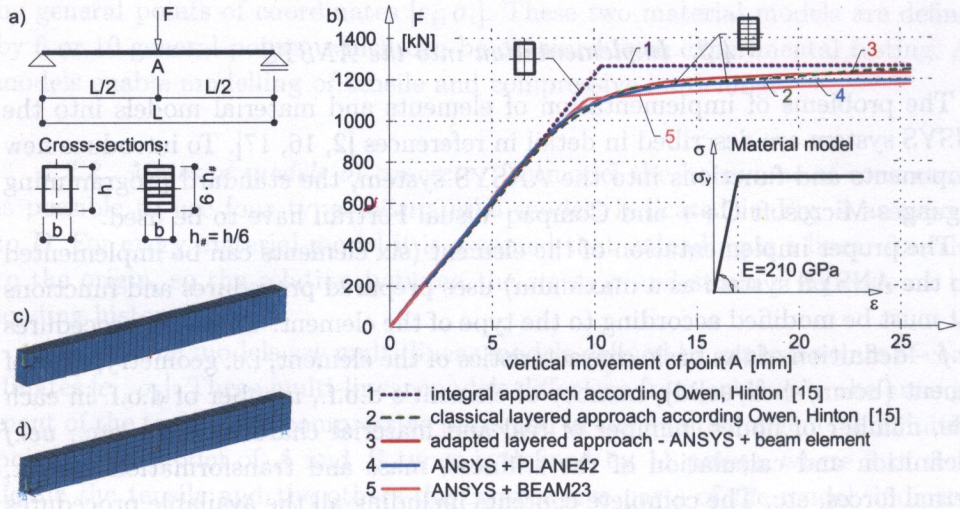

FIG. 5. Disposition of loading test (a), material model and load-displacement diagram (b), ANSYS models created using BEAM23 (c) and PLANE42 element (d).

The results are compared with those calculated using the integral and classical layered approach according to [15] and the standard ANSYS elements BEAM23 and PLANE42, Fig. 5. The same material characteristics, convergence criteria, load steps, etc. are used as in the calculation done by standard elements. A beam element internally divided also into six ($NL = 6$) layers is used in the classical layered approach described in [15].

Load-displacement diagram is shown in Fig. 5b. Load-displacement (l.d.) curve 1 shows that the girder fails as soon as a plastic hinge forms at the centre of the girder. More realistic results can be obtained using the layered approach, where yielding takes place gradually through the layers (smoother l.d. curves). Comparing l.d. curves 2 and 3, which are determined by the classical and adapted layered approach using [15] and ANSYS with beam element, we can declare a very good correspondence of the obtained results. It is also possible to find good agreement between the l.d. curves 3 and 4, e.g. ANSYS with beam element and ANSYS with PLANE42 element.

5.2. Example No. 2

Numerical example No. 2 describes the modelling of a simple bending test on the steel girder fixed at both ends, which is introduced in [15]. The fixed

girder of I shape cross-section $b \times h = 0.20 \times 0.20\,\mathrm{m}$, $c = 0.01\,\mathrm{m}$, $d = 0.02\,\mathrm{m}$ of span $L = 3.00\,\mathrm{m}$ is loaded along the beam length by vertical forces F (distance between two forces $x = 0.30\,\mathrm{m}$), the values of which are changed during the computation.

The height h of the cross-section is divided into 6 layers (top and bottom flange – 1 layer each, wall – 4 layers), Fig. 6, ($A_T = 0.002\,\mathrm{m}^2$). The real material behaviour is described as in [15] using the material model of type A without hardening ($E = 210\,\mathrm{GPa}$; $\mu = 0.3$; $\sigma_y = 250\,\mathrm{MPa}$). The results are compared as in example No. 1 with the results calculated using the integral and the classical layered approaches according to [15] and the standard ANSYS elements BEAM23, PLANE42 as well as SOLID45, Fig. 6.

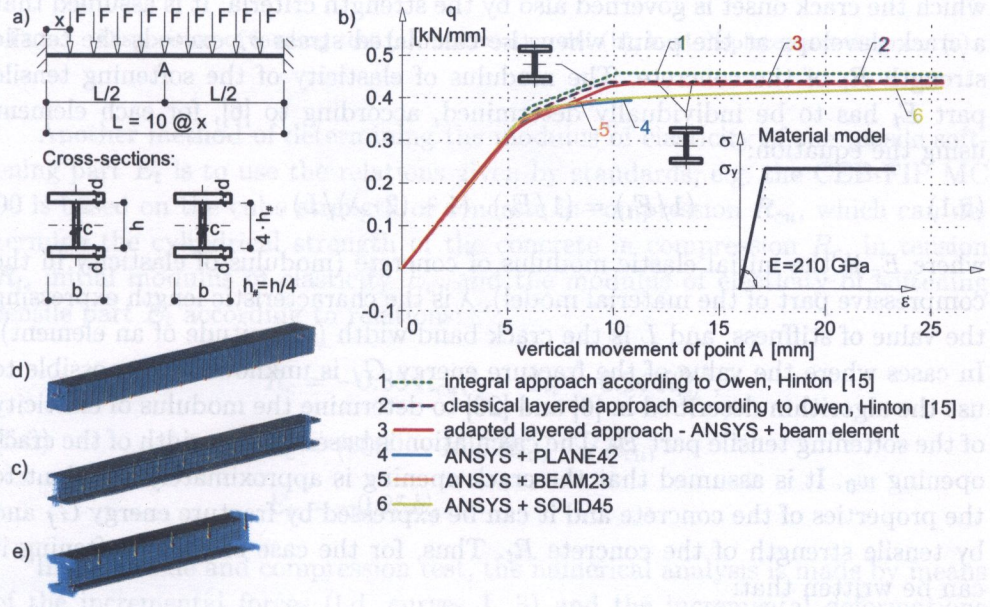

FIG. 6. Disposition of loading test (a), material model and load-displacement diagram (b), ANSYS models created using BEAM23 (c) and PLANE42 element (d).

The load-displacement diagram is shown in Fig. 6. L.d. curve 1 shows the loss of stiffness, which corresponds to the yielding of the end sections followed by a reduction when the central section becomes plastic, resulting in the girder failure mechanism. It is possible to get more realistic results, like those in example No.1, using the layered approach, where the yielding takes place gradually through the layers (smoother l.d.). Comparing l.d. curves 2 and 3, which are determined by the classical and adapted layered approaches using [15] and ANSYS with beam element, we can observe a very good agreement between the obtained results.

Comparison of these results with those obtained using ANSYS with BEAM23 or PLANE42 element is possible only at the initial part of load-displacement diagram. The results can be compared also with those obtained by means of the ANSYS with SOLID45 element (l.d. curve 6).

5.3. Example No. 3

Numerical example No. 3 describes modelling of an experimental test of tension and compression for a concrete specimen with dimensions $b \times h \times L = 0.10 \times 0.10 \times 0.40\,\mathrm{m}$. A material model with a linear softening tensile line is used for the calculation (type B), Fig. 4. Modulus of elasticity of the softening tensile part E_t of this material model is determined by the principle of fracture mechanics, in which the crack onset is governed also by the strength criteria. It is assumed that a crack develops at the point when the calculated stress σ_c exceeds the tensile strength R_t of the concrete. The modulus of elasticity of the softening tensile part E_t has to be individually determined, according to [6], for each element using the equation:

$$(1/E_t) = (1/E_c) \cdot (1 - (2 \cdot \lambda)/L)\,, \tag{5.1}$$

where E_c is the initial elastic modulus of concrete (modulus of elasticity in the compressive part of the material model), λ is the characteristic length expressing the value of stiffness, and L is the crack band width (magnitude of an element). In cases where the value of the fracture energy G_f is unknown, it is possible to use the algorithm described in [6] and [26] to determine the modulus of elasticity of the softening tensile part E_t. The calculation is based on the width of the crack opening w_0. It is assumed that the crack opening is approximately invariant to the properties of the concrete and it can be expressed by fracture energy G_f and by tensile strength of the concrete R_t. Thus, for the case of linear softening it can be written that:

$$w_0 = 2G_f/R_t = 0.000051\,m, \qquad \lambda = E_c\,G_f/R_t^2. \tag{5.2}$$

Calculation of the modulus of elasticity of the tensile softening part E_t is done using the initial elastic modulus, $E_c = 27.0$ GPa, the concrete tensile strength $R_t = 1.15$ MPa, and the concrete compressive strength $R_c = 11.0$ MPa. Inserting the input values into the Eq. (5.2) it is possible to determine the magnitude of fracture energy $G_f = 29.325$ N/m and also to define the magnitude of characteristic length $\lambda = 0.598$ m. If the characteristic length is known, then the length L of every element has to be found prior to the calculation of E_t. Let us consider the model being divided along its length with the average element length $L = 0.075$ m. Substituting it into the Eq. (5.1), the modulus of elasticity of the softening tensile part $E_t = 1.804$ GPa can be calculated, Fig. 7.

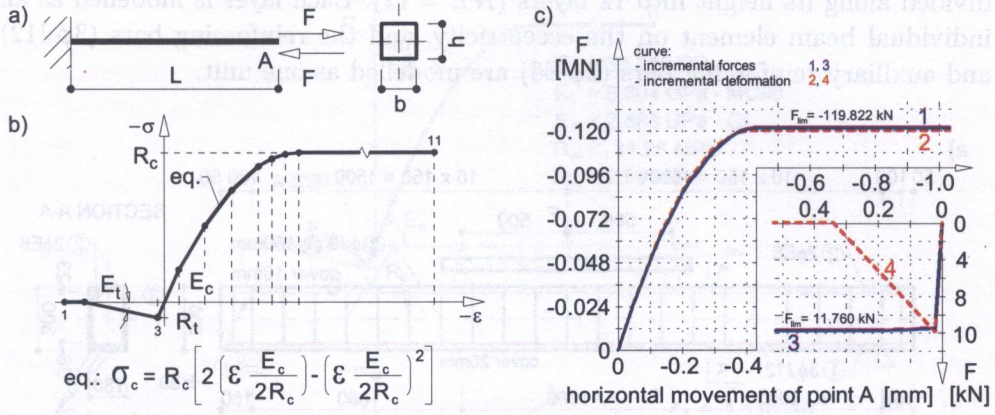

FIG. 7. Disposition of loading test (a), material model (b), load-displacement diagram (c).

Another method of determining the modulus of elasticity of the tensile softening part E_t is to use the relations given by standards, e.g. the CEB-FIP MC 90 is based on the cube strength of concrete in compression R_{cu}, which can determine the cylindrical strength of the concrete in compression R_c, in tension R_t, initial modulus of elasticity E_c, and the modulus of elasticity of softening tensile part E_t according to relations:

$$
\begin{aligned}
&R_c = -0.85\, R_{cu}, \qquad R_t = 0.24\, R_{cu}^{2/3}, \\
&E_c = (6000 - 15.5\, R_{cu}) \cdot \sqrt{R_{cu}}, \\
&E_t = -0.25 E_c.
\end{aligned}
\tag{5.3}
$$

In the tensile and compression test, the numerical analysis is made by means of the incremental forces (l.d. curves 1, 3) and the incremental deformations (l.d. curves 2, 4), Fig. 7.

5.4. *Example No. 4*

Numerical example No. 4 describes the modelling of experimental loading tests on reinforced girders with labels $G1$, $G2$ and $G3$. The tested girders are made from $B30$ concrete according to the code CSN 73 1201–86. The girders are reinforced in the tensile area by three reinforcing bars ϕJ12, and in the compressive area by two auxiliary reinforcing bars ϕE6, Fig. 8.

The model is formed by a simply supported girder with a span of $L = 3.00$ m and with overhanging ends 0.15 m in length, Fig. 8. The cross-sectional width is $b = 0.18$ m and the height $h = 0.30$ m. The cross-section in the model is

divided along its height into 12 layers ($NL = 12$). Each layer is modelled as an individual beam element on the eccentricity, and the reinforcing bars (3ϕ J12) and auxiliary reinforcing bars (2ϕ E6) are modelled as one unit.

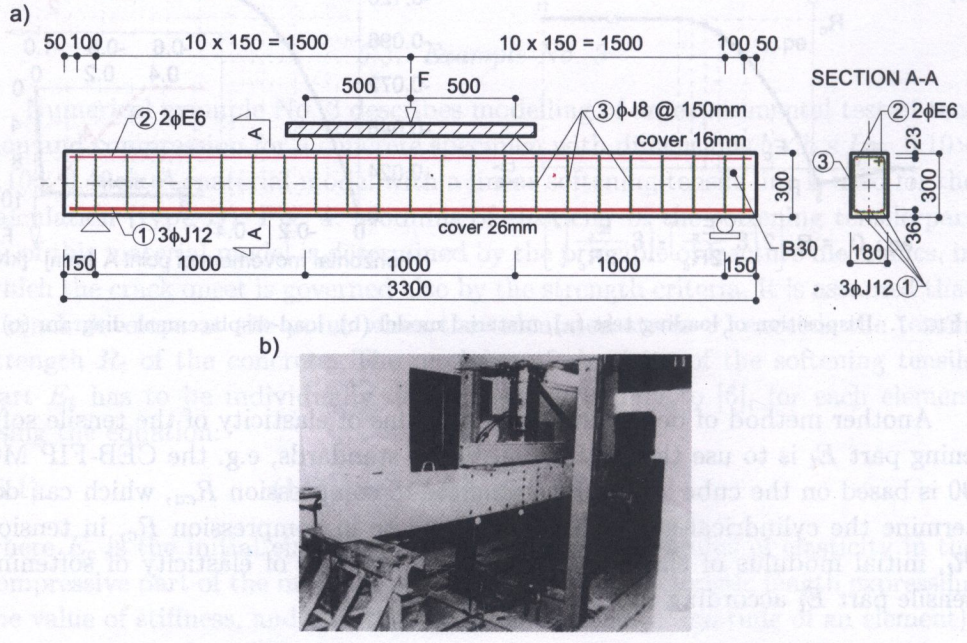

FIG. 8. Reinforcement diagram (a) and disposition of the loading test (b).

The material characteristics of the concrete and of the reinforcing bars are incorporated into the calculation with the help of material models, Fig. 9. For modelling of concrete behaviour, two material models of type B are used, Fig. 4, which differ from one another in the shape of the softening tensile part. For the first one, the modulus of elasticity of the softening tensile part is determined according to CEB-FIP MC 90 regulation ($E_t = 8.304$ GPa) and for the second one with the help of fracture energy G_f ($E_t = 2.868$ GPa), Fig. 9a. Definition points of the compressive part of the material models are determined with the help of experimentally obtained average cube strength of concrete ($R_{cu} = 31.96$ MPa) and initial elastic modulus of concrete ($E_c = 33.218$ GPa; $\mu = 0.15$). For modelling the reinforcing and auxiliary reinforcing bars, material models of type C are used, Fig. 5. The definition points of the material models are determined with the help of the following experimentally derived figures: average yield ($\sigma_y(J) = 368.40$ MPa; $\sigma_y(E) = 234.26$ MPa) and limit ($\sigma_p(J) = 579.20$ MPa; $\sigma_p(E) = 370.86$ MPa) stresses and initial modulus of steel ($E_s = 210$ GPa; $\mu = 0.3$), Fig. 9b.

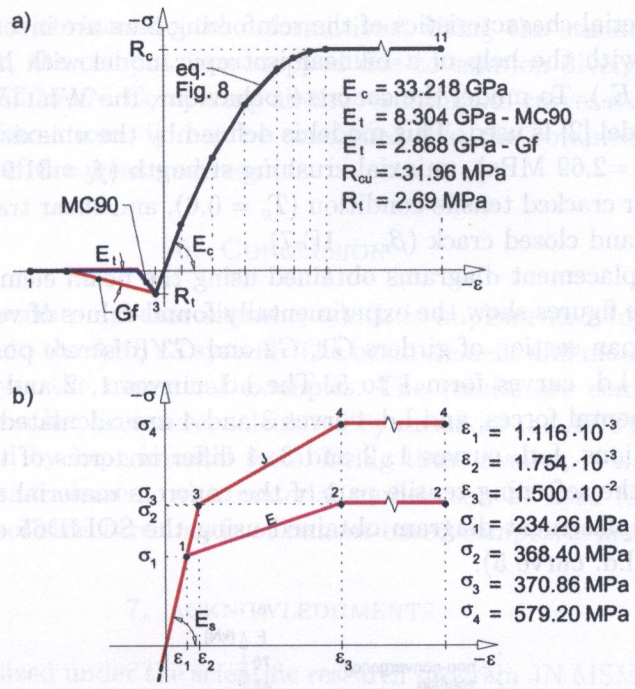

FIG. 9. Material models of concrete (a), material models of reinforcement (b).

The loading tests of reinforced girders are also modelled using the standard three-dimensional ANSYS concrete element SOLID65 with the same convergence criteria as in the case of the beam element. The calculation model is shown in Fig. 10. Except for the SOLID65 element, the SOLID45 and LINK8 elements are used. The LINK8 element is used for modelling the reinforcing bars (3ϕJ12), auxiliary reinforcing bars (2ϕE6) and stirrups (ϕJ8), Fig. 10b. The SOLID45 element is used for modelling the spread footing ($*$), the area under the spread footing ($\times$) and the bearing area ($+$), which are areas with a steep stress gradient, Fig. 10a.

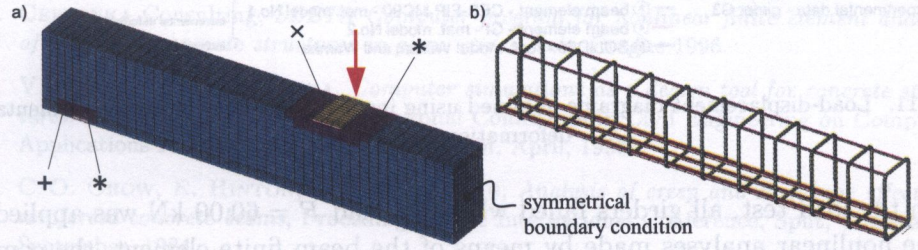

FIG. 10. Calculation model (half of the girder with symmetrical boundary condition) (a), reinforcing bars, auxiliary reinforcing bars and stirrups (b).

The material characteristics of the reinforcing bars are incorporated into the calculation with the help of a bilinear isotropic model with hardening (BISO; $E_H = 0.1 \times E_c$). To model the concrete behaviour, the WILLIAM and WARNKE material model [2] is used. This model is defined by the uniaxial tensile cracking strength (f_t =2.69 MPa), uniaxial crushing strength (f_c= 31.96 MPa), stiffness multiplier for cracked tensile condition ($T_c = 0.6$), and shear transfer coefficients for an open and closed crack (β_r = 1E-7).

Load-displacement diagrams obtained using the beam element are shown in Figs. 11. The figures show the experimentally found values of vertical deflections of the mid-span section of girders $G1$, $G2$ and $G3$ (discrete points) and numerically found l.d. curves form 1 to 5. The l.d. curves 1, 2 and 5 are calculated using incremental forces, and l.d. curves 3 and 4 are calculated using incremental deformations. L.d. curves 1, 2 and 3, 4 differ in terms of the magnitude of modulus of the softening tensile part of the concrete material model of type B. The load-displacement diagram obtained using the SOLID65 element is shown in Fig. 11a (l.d. curve 5).

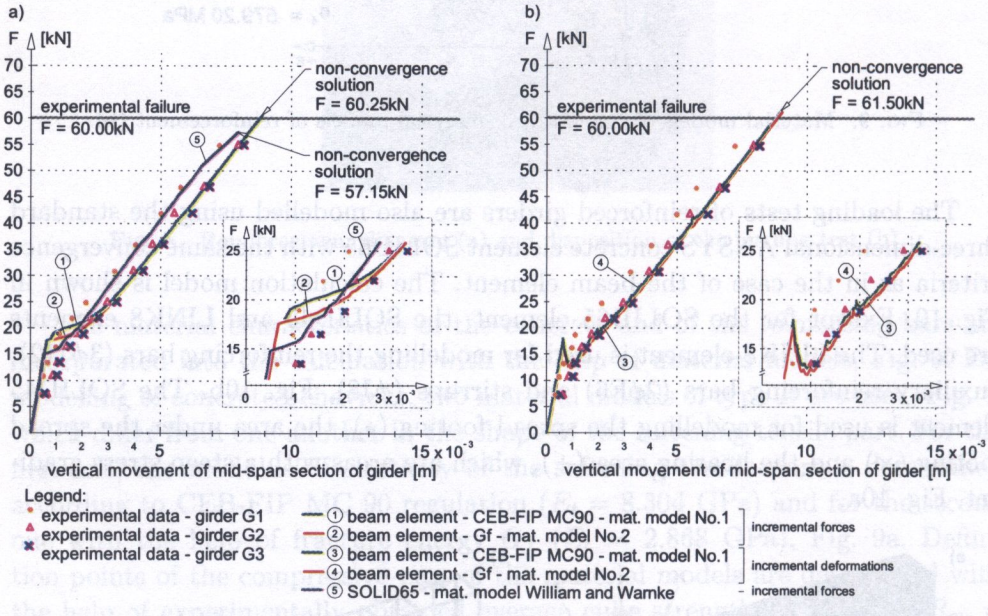

FIG. 11. Load-displacement diagrams obtained using incremental forces (a) and incremental deformations (b).

In the load test, all girders failed when the load $F = 60.00$ kN was applied. In the nonlinear analyses made by means of the beam finite element, the computation stopped due to solution divergence at the force action $F = 60.25$ kN when calculating with incremental forces, and at the force action $F = 61.50$ kN

when calculating with incremental deformations. Using the standard ANSYS SOLID65 element, the computation stopped due to solution divergence at the force action $F = 57.15$ kN. Comparing all the resulting l.d. curves with the measured vertical deformations, it may be concluded that the obtained results are within the limits of the measured results.

6. Conclusion

The paper describes a beam element, which is implemented together with material models into the ANSYS system. The beam element and material models are used to analyse the numerical examples. The results are compared with those published in other literature, calculated by means of the ANSYS standard elements, or found by experimental tests. Using these results, it is possible to claim that the beam element with material models can be used for nonlinear material analyses of structures made of cement-based composite materials.

7. Acknowledgments

The work was realized under the scientific research program JN MSM 261100007 and the grant project GACR 103/02/P083 "Development of finite elements for structural analysis from composite materials on cement base".

References

1. ANSYS Element Reference r. 5.5, Ansys, Inc., SAS IP, Inc., Houston, September 1998.
2. ANSYS Theory Reference r. 5.5, Ansys, Inc., SAS IP, Inc., Houston, September 1998.
3. www.ansys.com
4. K. J. Bathe, K. Jürgen, *Finite element procedures in engineering analysis*, Prentice-Hall Inc., ISBN 0–13–317305–4, 1982.
5. Z. J. Bittnar, J. Sejnoha, *Numericke metody mechaniky* (in Czech), Vol. 1, CVUT press, ISBN 80–01–00855–X, Prague 1992.
6. Cervenka Consulting, *SBETA Computer program for nonlinear finite element analysis of reinforced concrete structures in plane stress state*, Prague 1996.
7. V. Cervenka, J. Cervenka, *Computer simulations as a design tool for concrete structures*, ICCE-96, The Second International Conference in Civil Engineering on Computer Applications Research and Practice, Bahrain, April, 1996.
8. C. O. Chow, E. Hinton,A. H. H. Rahman, *Analysis of creep and shrinkage effects in reinforced concrete beams*, Procedings of the International Conference, Split, Yugoslavia, September, 1984.
9. M. A. Crisfield, *Nonlinear finite element analysis of solids and structures*, Vol. 1 Advanced Topics, John Wiley & Sons, 2001, ISBN 0–471–97059–X.

10. M. A. Crisfield, *Nonlinear finite element analysis of solids and structures*, Vol. 2 Advanced Topics, John Wiley & Sons, 2001, ISBN 0-471-95649-X.

11. B. L. Karihaloo, *Fracture Mechanics & Structural Concrete*, Longman Scientific & Technical, 1995, ISBN 0-582-21582-X.

12. V. Kolar, J. Kratochvil, F. Leitner, A. Zenisek, *Vypocet plosnych a prostorovych konstrukci metodou konecnych prvku* (in Czech), SNTL Praha 1979.

13. J. Navratil, *Casove zavisla analyza ramovych konstrukci* (in Czech), Stavebnicky casopis, **10**, 7, Slovac Academic Press, Bratislava 1992.

14. SCIA - nexis 32 - TDA manual (in Czech).

15. J. Owen, E. Hinton, *Finite elements in plasticity, Theory and practice*, Pineridge Press Limited, Swanseam, ISBN 0-906674-05-2, 1980.

16. J. Pencik, *Materially nonlinear analysis of concrete plane frame structures* (in Czech), PhD Thesis, Brno University of Technology, Brno 2001.

17. J. Pencik, *Ways of user modification of ANSYS* (in Czech), Vedecká konferencia, 226-229, TU Kosice, ISBN 80-7099-815-6, 2002.

18. F. G. Rammerstorfer, *Nonlinear analysis of shells by finite elements*, Springer Verlag, ISBN 0-387-82416-2, 1992.

19. A. H. H. Rahman, E. Hinton, *Linear and nonlinear finite element analysis of reinforced and prestressed concrete voided slabs*, Procedings of the International Conference, Split, Yugoslavia, September, 1984.

20. A. C. Scordelis, *Computer analysis of reinforced and prestressed concrete box girder bridges*, Procedings of the International Conference, Split, Yugoslavia, September, 1987.

21. A. C. Scordelis, *Computer models for nonlinear analysis of reinforced and prestressed concrete structures*, PCI Journal, 1985.

22. J. Strasky, J. Navratil, *Time-dependent analysis of the Wisconsin avenue viaduct*, Wisconsin, USA, 3rd International Kerensky Conference, Singapore 1994.

23. J. Strasky, P. Mikulastik, V. Jüttner, *Design of segmental structure with a cast-in-place deck slab*, *fib* Symposium 1999, Prague 1999.

24. A. Tessler, S. B. Dong, *On a hierarchy of conforming Timoshenko beam elements*, Computers & Structures, **14**, 3-4, 1981.

25. Technische Datenverarbeitung GmbH. TDV software - book of examples, example No. 6 Kao Ping HSI-Bridge, Taiwan 2000.

26. E. Vos, *Influence of loading rate and radial pressure on bond in reinforced concrete*, PhD Thesis, Delft University, 1983.

Received December 2, 2002; revised version January 12, 2004.